Intramolecular π–Stacking in Cationic Iridium(III) Complexes with Phenyl-Functionalized Cyclometalated Ligands: Synthesis, Structure, Photophysical Properties and Theoretical Studies

Peng Li,[a,b] Guo–Gang Shan,[b] Hong–Tao Cao,[b] Dong–Xia Zhu,*[b] Zhong–Min Su,*[a,b] Rukkiat Jitchati,[c,d] and Martin R. Bryce*[c]

[a] College of Chemistry, Jilin University, Qianjin Road 2699, Changchun 130023, P. R. China

[b] Institute of Functional Material Chemistry, Faculty of Chemistry, Northeast Normal University, Renmin Road 5268, Changchun 130024, P. R. China. Email: zhudx047@nenu.edu.cn, zmsu@nenu.edu.cn

[c] Department of Chemistry, Durham University, Durham DH1 3LE, U.K. Email: m.r.bryce@durham.ac.uk

[d] Chemistry Department, Ubon Ratchathani University, Warinchumrap, Ubon Ratchathani 34190, Thailand

Keywords: Iridium / Luminescence / Photophysics / Density functional calculations / Light-emitting cells

Abstract

The syntheses of two new heteroleptic cationic iridium complexes containing 2,6–diphenylpyridine (Hdppy) and 2,4,6–triphenylpyridine (Htppy) as the cyclometalated ligands, namely [Ir(dppy)$_2$phen]PF$_6$ (**1**) and [Ir(tppy)$_2$phen]PF$_6$ (**2**) (phen is 1,10–phenanthroline), are described. The X-ray crystal structure of **2** reveals a distorted octahedral geometry around the Ir center and close intramolecular face-to-face π–π stacking interactions between the pendant phenyl rings at the 2-position of the cyclometalated ligands and the N^N ancillary ligand. This represents a new mode of π–π stacking in charged Ir complexes. Complexes **1** and **2** are green photoemitters: their photophysical and electrochemical properties are interpreted with the assistance of density functional theory (DFT) calculations. These calculations also establish that the observed intramolecular interactions cannot effectively prevent the lengthening of the Ir–N bonds of the

complexes in their metal-centered (^{3}MC) states. Complexes **1** and **2** do not emit light in light-emitting electrochemical cells (LECs) under conditions in which the model compound [Ir(ppy)$_2$phen]PF$_6$ **3** emits strongly. This is explained by degradation reactions of the ^{3}MC state of **1** and **2** under the applied bias during LEC operation facilitated by the enhanced distortions in the geometry of the complexes. These observations have important implications for the future design of complexes for LEC applications.

Introduction

Cyclometalated Ir(III) complexes have attracted considerable attention during the last decade due to their synthetic versatility, high thermal stability, relatively short excited state lifetime, high photoluminescence efficiency and good emission wavelength tunability.[1] They have been widely exploited as emitters in phosphorescent organic light emitting diodes (PhOLEDs),[2,3] solid-state lighting[4] and light-emitting electrochemical cells (LECs).[5] LECs offer advantages over conventional OLEDs due to their simpler device architecture, the use of spin-coating techniques in their fabrication and the use of air–stable electrodes without the need for rigorous encapsulation, all of which are applicable to large-area emission and cheap processing. In LECs ionic transition metal complexes (iTMCs) of the generic formula [(C^N)$_2$Ir(N^N)$^+$PF$_6^-$] perform all the roles needed to generate light.[6] When an electrical bias is applied to the LEC, the iTMCs serve to (i) decrease the injection barriers via the displacement of the counterions; (ii) transport the electrons and holes via consecutive reduction and oxidation processes, and (iii) generate the photons. The devices can operate at very low voltages, yield high brightness and power efficiency and tunable emission color.

The practical applications of iTMC-based LECs are hampered by current limitations in their stability.[7] Nucleophile–assisted ligand–exchange reactions at the metal center can occur and the new complex that is formed can quench the luminescence. A strategy initiated by Bolink, Constable et al. which involves shielding the Ir atom of the iTMC by intramolecular $\pi-\pi$ stacking (forming "an intramolecular cage"[6a]) has led to dramatic improvements in stability and enhanced lifetimes of the LECs.[8] For this purpose phenyl groups have been attached at the positions *alpha* to nitrogen on the N^N ancillary ligands. For example, pendant phenyl group(s) on bpy (2,2'–bipyridine), phen (1,1–phenanthroline) and pzpy [2–(1–*H*–pyrazol–l–yl)pyridine] ligands

engage in face-to-face intramolecular π–π stacking interactions with the cyclometalating C^N ligands.[8,9] These interligand interactions effectively close the complexes in the ground states (S_0), the emitting (T_1) states and the metal–centered (^{3}MC) triplet excited states and thereby protect the complexes from attack by nucleophiles such as water.[8b]

Similarly, our group has reported cationic Ir(III) complexes based on the 2–(5–phenyl–2–phenyl–2H–1,2,4–triazol–3–yl)pyridine (Phtz) ancillary ligand which also show intramolecular π–π interactions. Density functional theory (DFT) calculations clearly indicated that these interactions reduced the possibility of the ligand–exchange degradation reactions.[10] We note that Duan et al reported that phenyl substitution on the N-heterocyclic carbene ancillary ligand of [Ir(ppy)$_2$(pyphmi)]PF$_6$ (Hppy = 2-phenylpyridine, pyphmi = 3-phenyl-1-(2-pyridyl)imidazolin-2-ylidene-C,C$^{2'}$) leads to weak π–π interactions and increased torsion angles which do not enhance the stability of the LECs.[5g]

To the best of our knowledge, the π–stacking strategy has exclusively involved pendant phenyl substitution on the ancillary ligand.[8-11] The aim of the present work is to address a fundamental question: What is the effect of attaching pendant phenyl substituents *to the cyclometalating (C^N) ligands*? We now present the synthesis and characterization of two new complexes [Ir(dppy)$_2$(phen)][PF$_6$] (**1**) and [Ir(tppy)$_2$(phen)][PF$_6$] (**2**) (Figure 1) where Hdppy, Htppy and phen are 2,6–diphenylpyridine, 2,4,6–triphenylpyridine and 1,10–phenanthroline, respectively. An X–ray crystal structure analysis of **2** shows strong intramolecular π–π stacking interactions. The photophysical and electrochemical properties of **1** and **2** are reported, along with DFT/TD-DFT calculations. LECs have been fabricating using complexes **1** and **2**. Data are compared with the archetypal parent complex [Ir(ppy)$_2$(phen)][PF$_6$] (**3**) which serves as a reference.

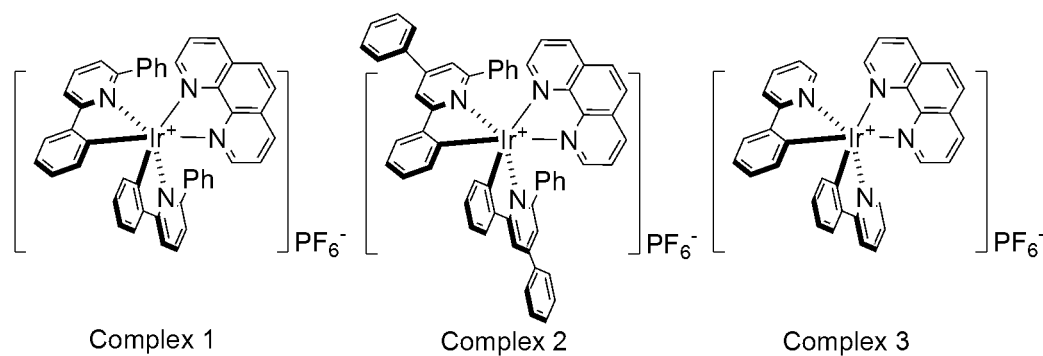**Figure 1.** Chemical structures of complexes **1** and **2** and the parent complex **3**, which is included for comparison.

Results and discussion

Synthesis. The synthesis of complexes **1** and **2** (Figure 1) followed the standard routes for complexes of the generic formula $(C^\wedge N)_2Ir(N^\wedge N)^+PF_6^-$. The low yield for the formation of **1** and **2** is due to the steric hindrance from the *o*-phenyl substituents, as observed previously with sterically-hindered C^N ligands.[12] The complexes were unambiguously characterized by ^{1}H NMR spectroscopy, mass spectrometry and elemental analysis.

X–ray Crystal Structure of Complex 2. The solid state structure of **2** was determined by single crystal X–ray diffraction. As depicted in Figure 2, complex **2** adopts a distorted octahedral geometry around the Ir center.

Figure 2. The X-ray molecular structure of the cation in complex **2** including the centroid-to-centroid distances.

The structure is characterized by the small bite angle C(3)–Ir(1)–N(1) (80.48°), C(3A)–Ir(1)–N(1) (80.48°), N–Ir(1)–N(OA) (75.57°), and twisted bond angles of C(3)–Ir(1)–N (169.59°), C(3A)–Ir(1)–N(OA) (169.59°), N–Ir(1)–N(OA) (172.19°). The Ir–N(phen) (2.209 Å), Ir–C(tppy) (2.005Å), Ir–N(tppy) (2.074 Å) distances of complex **2**, closely resemble those previously reported for the parent complex [Ir(ppy)$_2$(phen)][PF$_6$] **3**: Ir–N(phen) (2.137, 2.150 Å), Ir–C(ppy) (2.003, 2.017 Å), Ir–N(ppy) (2.043, 2.048 Å)].[8c] However, there are small differences

in some of the bond lengths between structures **2** and **3** as a consequence of the steric interactions of the pendent phenyl groups in complex **2**. Specifically for complex **2** [Ir–N(tppy) ~2.074 Å, Ir–N(phen) ~2.209 Å] are slightly longer than the comparable bonds in **3** [Ir–N(ppy) ~2.05 Å, Ir–N(phen) ~2.14 Å].[8c] Figure 2 illustrates the double face–to–face π–stacking between the pendant phenyl ring of both tppy ligands and the ancillary phen ligand of **2**; the interaction is in an optimal offset arrangement at a separation (centroid–to–centroid) of 3.276 Å. This stacking distance is similar to those observed in the [Ir(ppy)$_2$(pbpy)]$^+$ and [Ir(ppy)$_2$(dpbpy)]$^+$ cations (pdpy and dpbpy are 6-phenyl-2,2-bipyridine and 6,6'-diphenyl-2'2-bipyridine, respectively).[8b] This observation confirms that the intramolecular caged structure is formed by introducing a pendant phenyl group at C(2) of the cyclometalating ppy unit.

Photophysical properties

The absorption and emission spectra of complexes **1** and **2** were recorded in degassed acetonitrile solutions at room temperature as shown in Figure 3. The photophysical characteristics are reported in Table 1. The strong absorption bands in the range of 200–350 nm are assigned to spin–allowed π–π* transitions from the ligands. The relatively weak absorption bands that occur in the lower energy region (350–500 nm) correspond to ^{1}MLCT (metal–to–ligand charge–transfer), ^{3}MLCT, ^{1}LLCT (ligand–to–ligand charge–transfer), ^{3}LLCT, and ligand–centered (LC) ^{3}π–π* transitions with reference to that reported for other Ir(III) complexes.[13] This observation implies that the spin–forbidden ^{3}MLCT, ^{3}LLCT and LC ^{3}π–π* transitions have gained considerable intensity via mixing with the higher–lying spin–allowed ^{1}MLCT transitions because of the strong spin–orbit coupling endowed by the iridium atom. Generally, for cationic Ir(III) complexes, there are three excited states, namely ^{3}MLCT, ^{3}LLCT and LC ^{3}π–π*, contributing to light emission.[14] At room temperature, **1** and **2** exhibit intense green emission with peak values at 546 and 552 nm, respectively, in CH$_3$CN solutions. The broad and featureless bands indicate that the emissive excited states of these two complexes are predominantly ^{3}MLCT or ^{3}LLCT in character, rather than LC ^{3}π–π* transitions which typically show vibronic structure in the emission spectra.[15] Upon cooling the CH$_3$CN solutions to 77 K, the emission spectra of **1** and **2** remain broad and are blue shifted indicating that, at low temperature, their excited states retain ^{3}MLCT and ^{3}LLCT character.[14]
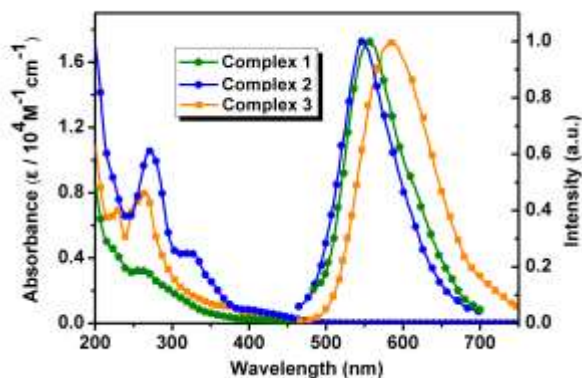
Figure 3. Absorption and normalized emission spectra of complexes **1**, **2** and **3** in CH$_3$CN solutions at room temperature.

As shown in Figure 3, the 2–phenyl substituents cause a significant blue shift in the emission wavelengths of complexes **1** and **2** (31 and 37 nm, respectively) compared to complex **3**. The further blue shift for complex **2** is ascribed to the additional electron-donating phenyl group at C(4) of the pyridyl ring.[16] The emission for complex **3** (λ_{max} 583 nm in MeCN; Figure 2) is consistent with previously reported data for this complex (579 nm in MeCN;[17] 575 nm in CH$_2$Cl$_2$).[18] The emission spectra for **1-3** have the same trend in a non-coordinating solvent such as CH$_2$Cl$_2$ (see Figure **S5** in Supporting Information).

Table 1. Photophysical and electrochemical data for complexes 1 and 2.

	PL at room temperature						PL at 77 K^a	Electrochemical data^a	
	$\lambda_{em}{}^a$ [nm]	$\Phi_{PL}{}^b$ [τ (μs)]^a	$k_r{}^{a,c}$ [$\times 10^5$]	$k_{nr}{}^{a,c}$ [$\times 10^6$]	$\lambda_{em}{}^d$ [nm]	$\Phi_{film}{}^d$	λ_{em} [nm]	E_{ox} [V]	E_{red} [V]
Complex **1**	552	0.15 (0.23)	6.6	3.71	595	0.06	515, 552sh	0.80	-1.58
Complex **2**	546	0.06 (0.31)	2.0	3.06	552	0.10	517, 545sh	0.80	-1.59
Complex **3**	583	0.39 (0.23)	17.3	2.71	591	0.11	532	0.79	-1.58

^{a} Data obtained in acetonitrile solution; λ_{exc} 355 nm. ^{b} Estimated error of $\pm$10%. ^{c} $k_r=\Phi_{PL}\times\tau^{-1}$. ^{d} Data obtained in neat thin film.

For complexes **1** and **2**, the PLQYs are 0.15 and 0.06 in CH$_3$CN solutions, respectively. Complex **1** shows a significantly higher radiative rate constant than **2**, which may be the reason that **1** has a higher PLQY in solution, as the non-radiative rate constants for both **1** and **2** are quite similar. Conversely, in thin films the PLQY of **2** (Φ 0.10) is higher than for **1** (Φ 0.06) as the steric

bulk of the extra phenyl substituent now has the beneficial effect of reducing self-quenching. The excited-state lifetimes of **1** and **2** in solution are 0.23 μs and 0.31 μs, respectively, which is typical for phosphorescent emission in $(C\wedge N)_2Ir(N\wedge N)^+PF_6^-$ complexes.[8] The radiative decay rate (k_r) of **1**-**3** in CH_3CN solution were calculated (6.6×10^5 for **1**, 2.0×10^5 for **2**, and 17.3×10^5 for **3**).

Electrochemical properties

The electrochemical behavior of complexes **1** and **2** was investigated by cyclic voltammetry in CH_3CN solutions and data are reported vs ferrocene/ferrocenium in Table 1. The complexes **1** and **2** exhibit a quasi-reversible oxidation and reduction peaks at E_{ox} 0.80 V and E_{red} −1.58 / −1.59 V, respectively, which are very similar to the data obtained under the same conditions for complex **3** [(0.79 and −1.58 V (this work) (cf. 0.85 and −1.54 V in CH_2Cl_2)].[19] These data are consistent with the oxidation occurring primarily on the Ir and the phenyl ring of the cyclometalated ligand, whereas the reduction is localized on the ancillary ligand.

Quantum chemical calculations

The geometries and electronic structures of complexes **1** and **2** were calculated using DFT/TDDFT methods at the B3LYP/(6-31G*+LANL2DZ) level to provide additional insights into the structures and nature of the emissive excited states. Figure 4 displays the atomic orbital compositions of the lowest unoccupied and highest occupied molecular orbitals (LUMO and HOMO, respectively) of the cations of **1** and **2**. The LUMO of both complexes is almost the same, residing on the phenanthroline group. The HOMO is composed of a mixture of π−orbitals on the phenyl group at C(2) of the cyclometalated ligands and iridium d orbitals: the phenyl groups at C(4) or C(6) make no contribution to the HOMOs. These data are consistent with studies on analogous complexes.[8] To further understand the emission processes of **1** and **2**, TD-DFT methods were used to calculate the low lying triplet states (T_1) at the optimized geometry of the ground state (S_0). The orbital diagrams show that the T_1 state for complex **1** mainly originates from HOMO → LUMO (74%), and the T_1 state for **2** mainly originates from HOMO → LUMO+1 (56%) and HOMO → LUMO+3 (20%) transitions (Fig. S6). These data suggest that the lowest excited states are induced by ³MLCT (iridium → ancillary ligand) with some ³LLCT character (cyclometalated ligands → phen). In addition, the unpaired-electron spin density distribution calculated for complexes **1** and **2**

perfectly matches the topology of the HOMO→LUMO excitation in which the T_1 state originates and confirms the mixed ^{3}MLCT/^{3}LLCT character of the lowest triplet state (Fig. S7).[8d] The photophysical properties and the calculated results illustrate that the emission of **1** and **2** mainly originates from the T_1 states which agrees with the experimentally observed broad unstructured emission spectra of both complexes (Figure 3).
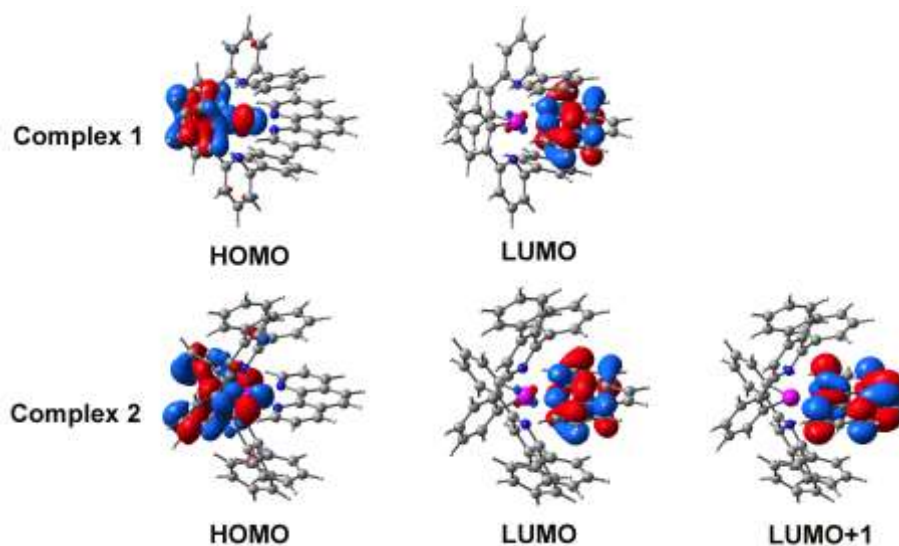

Figure 4. HOMO and LUMO distributions of complexes **1** and **2**.

The metal-centered (^{3}MC) states result from the excitation of an electron from the occupied t_{2g} (dπ) HOMO to the unoccupied e_{2g} (dσ*) level, which is regarded as the origin of the degradation process for Ru(II)- and Ir(III)-based LECs.[7] In the ^{3}MC states, the rupture of metal-ligand bonds can induce opening of the structure and thereby enhance the reactivity of complex; thus photodegradation is facilitated and the device becomes unstable. The robust intramolecular π–stacking observed in the complexes reported by Bolink et. al. minimizes the expansion of the metal-ligand bonds in the excited state and this prevents the unwanted ligand exchange reactions.[8] To evaluate the stability of complexes **1** and **2**, the molecular structures of the ^{3}MC states were fully optimized from the minimum energy structure of S_0 with Ir–N$_{ppy}$ bond distances lengthened to 2.70 Å.[8h] The metal-centered character of the triplet states for complexes **1** and **2** was confirmed by the spin densities, which were calculated for the optimized ^{3}MC state geometries. The spin densities are mainly concentrated on the iridium atom, with 1.47 eV unpaired electrons for both complexes **1** and **2** in their ^{3}MC states. The key bond lengths that affect the stabilities of

complexes **1** and **2** in the ^{3}MC states are presented in Figure 5. The Ir-N$_{phen}$ bond lengths are 2.23 Å for **1** and **2** in the ^{3}MC state which is similar to the Ir-N$_{phen}$ bond lengths (2.26 Å) in T$_1$. The structures show that the face-to-face π-stacking, as observed in the X-ray crystal structure of **2** (Figure 2) is retained in the ^{3}MC states with centroid-to-centroid distances of 4.006 Å and 4.022 Å for **1** and **2**, respectively.
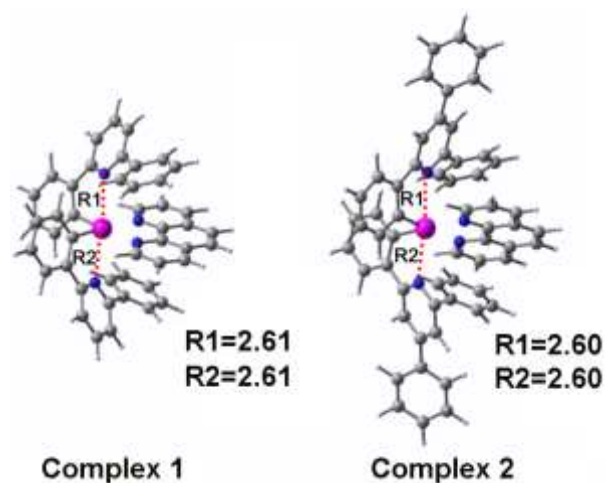

Figure 5. Minimum–energy structures calculated for the ^{3}MC states of complexes **1** and **2**. Distances R1 and R2 are the optimized Ir–N$_{cyclometalated\ ligand}$ bond lengths (Å).

However, a crucial point is that unlike the iridium complexes with a pendant phenyl group on the ancillary ligand, e.g. [Ir(ppy)$_2$(pbpy)]$^+$,[8b] in complexes **1** and **2** the intramolecular π-π interactions do *not* prevent opening of the structure in the ^{3}MC state. For example, as shown in Figure 5, the calculated Ir–N bond lengths (R1 and R2) of **1** increased from 2.13 Å in the ground state (S$_0$) to 2.61 Å in the ^{3}MC state, which are the same changes as in complex **2**. Complex **3** exhibits similar changes to the corresponding bond lengths (Figure S8).

Light-emitting Cells (LECs)

To investigate the electroluminescent properties of the complexes, LECs were prepared with a structure of ITO/PEDOT:PSS (50 nm)/iridium complex : IL (molar ratio 4:1 w/w) (75 nm)/Al (120 nm). [PEDOT:PSS is (poly(3,4-ethylenedioxythiophene)：poly(styrene sulfonate)]; IL is the ionic liquid 1-butyl-3-methylimidazolium hexafluorophosphate (BMIMPF$_6$)] which is known to reduce drastically the turn-on time of LECs and to enhance the ionic conductivity of the thin film.[20] This is the standard LEC architecture which our groups have used previously.[21] As a benchmark,

model complex **3** was studied in the present work. As expected, upon applying a bias of 3 V to the device using complex **3** light emission was observed within a few minutes, as reported previously by us[19] and by Bolink et al[8c] for this complex. However, for complexes **1** and **2**, under identical conditions *no light emission was observed* even after applying a bias of 3 V for as long as 24 h. Moreover, at a higher bias (8 V) for 24 h no light emission was observed. These studies demonstrate that although complexes **1** and **2** show efficient photoluminescence they are not suitable for LECs. This can be explained by the distorted molecular structure induced by the double π–stacking (as revealed by X-ray analysis) and by the theoretical calculations which show that the intramolecular π–π interactions in **1** and **2** are not effective in preventing the transition to a more open structure with an expanded Ir–N coordination sphere in the excited states. Consequently, we conclude that the double π–stacking in complexes **1** and **2** is detrimental to stability and it is likely that the complexes degrade in the excited state by reactions with adventitious nucleophiles and so luminescence is quenched.

Conclusion

This combined experimental and theoretical study has provided new insights into the established strategy of using intramolecular π–π stacking in cationic Ir(III) complexes to enhance LEC performance. Complexes **1** and **2** possess the novel feature of pendant phenyl rings *alpha* to the nitrogen of the cyclometalating units. X-ray analysis of **2** shows a distorted octahedral geometry with strong intramolecular face–to–face π–π stacking interactions between the pendant phenyl units and the ancillary ligands. DFT calculations establish that the intramolecular interactions are retained in the excited triplet states and that this mode of π–π stacking does not prevent the opening of the Ir–N coordination sphere in the excited states. Consequently, although the complexes are photoluminescent, they do not emit light in LECs under conditions in which the model compound [Ir(ppy)$_2$phen]PF$_6$, emits strongly. This is presumably because of degradation reactions of the ^{3}MC state of **1** and **2** under the applied bias during LEC operation. This combined experimental and theoretical study provides new insights into structure/property relationships in ionic Ir complexes and demonstrates convincingly that in specific cases intramolecular π–π stacking can be detrimental to LEC performance due to enhanced distortions in the geometry of the complex. This is valuable information for the future design of complexes for LEC applications.

Experimental section

Materials, synthesis and characterization

All reagents and solvents employed were commercially available and used as received without further purification. The solvents for syntheses were freshly distilled over appropriate drying reagents. All experiments were performed under a nitrogen atmosphere by using standard Schlenk techniques. ^{1}H NMR spectra were measured on Bruker Avance 500 MHz with tetramethylsilane as the internal standard. Mass spectra were recorded using matrix–assisted laser desorption–ionization time–of–flight (MALDI–TOF) mass spectrometry. Elemental analyses (C, H, and N) were obtained using a Perkin-Elmer 240C elemental analyzer. UV−vis absorption spectra were recorded on a Hitachi U3030 spectrometer. The emission spectra were recorded using the F–7000 fluorescence spectrophotometer. The excited–state lifetime was measured on a transient spectrofluorimeter (Edinburgh FLS920) with a time–correlated single–photo–counting technique. The photoluminescence quantum yields (PLQYs) in solution and in neat film were measured with an integrating sphere in a fluorospectrophotometer. Cyclic voltammetry was performed on a BAS 100 W instrument with a scan rate of 100 mV s^{-1} in CH$_3$CN with the three–electrode configuration: a glassy–carbon electrode as the working electrode, an aqueous saturated calomel electrode as the pseudo–reference electrode, and a platinum wire as the counter–electrode. A 0.1 M solution of tetra-n-butylammonium perchlorate (TBAP) in CH$_3$CN was used as the supporting electrolyte and ferrocene was selected as the internal standard.

Synthesis. Ligands Hdppy[12] and Htppy[12] and complex **3**[17] were synthesized as described in the literature. The bridged μ-dichloro diiridium C^N ligand complexes, which are precursors to complexes **1** and **2**, were synthesized from Hdppy and Htppy, respectively, following standard literature procedures for analogs.[22]

[Ir(dppy)$_2$(phen)](PF$_6$) (1). A mixture of 2,6-diphenylpyridine (508 mg, 2.2 mmol), IrCl$_3$·3H$_2$O (352 mg, 1.0 mmol) 2-ethoxyethanol (12 mL) and water (4 mL) was heated at 120 ^{o}C. After 12 h the mixture was cooled to 20 ^{o}C, filtered and the precipitate was washed with water then dissolved in CH$_2$Cl$_2$. The organic solution was separated, dried over MgSO$_4$, filtered and evaporated to give a pale green solid, presumed to be the bis–μ–chloro-bridged complex, which was used directly in the next step. A mixture of this complex (138 mg, 0.1 mmol) and phenanthroline (36 mg, 0.2 mmol) in dichloromethane (30 mL) and methanol (15 mL) was heated under reflux for 24 h in the dark.

After cooling to room temperature, the mixture was filtered, then an excess of solid KPF_6 was added and the mixture stirred for 1 h at room temperature. The solvent was removed under reduced pressure and the residue was purified by silica gel column chromatography using a mixture of dichloromethane/ethyl acetate (4:1, *v/v*) as eluent to yield complex **1** (8 mg) as a yellow solid. ^{1}H NMR (500 MHz, CDCl$_3$, δ [ppm]): 8.20 (d, *J* = 7.5 Hz, 2H), 8.02 (d, *J* = 7.5 Hz, 2H), 7.98 (s, 2H), 7.88 (d, *J* = 7.5 Hz, 2H), 7.63–7.67 (m, 4H), 7.20–7.24 (m, 6H), 7.02 (t, *J* = 7.5 Hz, 2H), 6.81 (d, *J* = 8 Hz, 2H), 6.62 (t, *J* = 3.5 Hz, 4H), 6.48 (d, *J* = 8 Hz, 2H), 6.11 (s, 2H), 5.01 (d, *J* = 7 Hz, 2H). Anal. calcd for $C_{48}H_{36}F_6IrN_4P$: C, 57.31; H, 3.61; N, 5.57. Found: C, 57.36; H, 3.65, N, 5.61%. ESI–MS: m/z 833.2 (M–PF$_6$).

[Ir(tppy)$_2$(phen)](PF$_6$) (2). Following the same procedure as for complex **1**, 2,4,6-triphenylpyridine (676 mg, 2.2 mmol) gave a pale green solid, presumed to be the bis–μ–chloro-bridged complex, which was used directly in the next step. A mixture of this complex (168 mg, 0.1 mmol), phenanthroline (36 mg, 0.2 mmol) in dichloromethane (30 mL) and methanol (15 mL) was heated under reflux for 24 h in the dark. Work-up and purification as described for complex **1**, yielded **2** (15 mg). ^{1}H NMR (500 MHz, DMSO–d$_6$, δ [ppm]): 8.69 (d, *J* = 1.5 Hz, 2H), 8.37–8.42 (m, 4H), 8.07 (s, 2H), 7.98–8.00 (m, 4H), 7.67 (d, *J* = 4 Hz, 2H), 7.48–7.50 (m, 8H), 7.17–7.22 (m, 4H), 7.03–7.06 (m, 2H), 6.96 (d, *J* = 2 Hz, 2H), 6.84 (d, *J* = 7.5 Hz, 2H), 6.64 (t, *J* = 7.5 Hz, 2H), 6.56 (t, *J* = 7.5 Hz, 2H), 6.06 (t, *J* = 7.5 Hz, 2H), 5.11 (d, *J* = 7.5 Hz, 2H). Anal. calcd for $C_{60}H_{44}F_6IrN_4P$: C, 62.22; H, 3.83; N, 4.84. Found: C, 62.27; H, 3.91, N, 4.88%. ESI–MS: m/z 983.2 (M–PF$_6$). Single crystals of complex **2** were obtained by slow evaporation of a dilute CH$_2$Cl$_2$ solution of the complex.

X–Ray Crystallography. Data collection for complex **2** was performed on a Bruker Smart Apex II CCD diffractometer with graphite–monochromated Mo Kα radiation (λ = 0.71069 Å) at 293 K. Absorption corrections were performed by using the multi–scan technique. The crystal structure was solved by Direct Methods of SHELXTL–97[23] and refined by full–matrix least–squares techniques using SHELXTL–97 within WINGX.[24] The hydrogen atoms of the aromatic rings were included in the structure factor calculation at idealized positions by using a riding model. Anisotropic thermal parameters were used to refine all non–hydrogen atoms except for some of the nitrogen and carbon atoms. Structural data in CIF format is available as Supporting Information or from the Cambridge Structural Database (CCDC-956631).

Theoretical Calculations. The ground and excited electronic states of the complexes were investigated by performing DFT and TD–DFT calculations at the B3LYP level.[25] The 6-31G* basis sets were employed for optimizing the C, H, N atoms and the LANL2DZ basis sets for the Ir atom. An effective core potential (ECP) replaces the inner core electrons of iridium leaving the outer core $(5s)^2(5p)^6$ electrons and the $(5d)^6$ valence electrons of Ir(III). The geometry of the metal–centered triplet (^{3}MC) was fully optimized and was calculated at the spin–unrestricted UB3LYP level with a spin multiplicity of **3**. All calculations reported here were carried out with the Gaussian 09 software package.[26]

Device Preparation and Characterization. PEDOT:PSS is poly(3,4-ethylenedioxythiophene):poly(styrenesulfonate) (CLEVIOS^{TM} P VP Al 4083 aqueous dispersion, 1.3-1.7% solid content Heraeus); solvents were obtained from Aldrich. Indium tin oxide (ITO)-coated glass substrates (20 $\Omega/\square^2$) were cleaned and treated with oxygen plasma before use. The PEDOT:PSS layer was spin-coated onto the ITO substrate and baked at 100 ^{o}C for 30 min, yielding a film with a thickness of ca. 100 nm. After cooling to room temperature, the solutions of complexes **1–3** and the ionic liquid 1-butyl-3-methylimidazolium hexafluorophosphate (BMIMPF$_6$) in CH$_2$Cl$_2$ were spin-coated onto the substrate, and then the layer with a thickness of ca 90 nm was baked at 80 ^{o}C for 2 h. The film was transferred into a metal evaporating chamber where an aluminum cathode (120 nm) was evaporated under low pressure ($<5\times10^{-4}$ mbar). The EL spectra were obtained with a Photo Research PR650 spectrophotometer in ambient conditions by applying a constant voltage using a Keithley 2400 source meter.

Supporting Information

Supporting information for this article is available on the WWW under http://dx.doi.org/10.1002/ejic. The SI includes: ^{1}H NMR spectra of **1** and **2**; cyclic voltammograms of **1-3**; theoretical calculations of **1-3**; emission spectra of **1-3** in solution.

Notes and References

[1] a) V. W-W. Yam, K. M-C. Wong, *Chem. Commun*. **2011**, *47*, 11579; b) J. D. Routledge, A. J. Hallett, J. A. Platts, P. N. Horton, S. J. Coles, S. J. A. Pope, *Eur. J. Inorg. Chem*. **2012**, 4065.

[2] H. Yersin, (Ed.), *Highly Efficient OLEDs with Phosphorescent Materials*; Wiley-VCH, Weinheim, **2008**.

[3] K. Walzer, B. Maennig, M. Pfeiffer, K. Leo, *Chem. Rev*. **2007**, *107*, 1233.

[4] K. T. Kamtekar, A. P. Monkman, M. R. Bryce, *Adv. Mater*. **2010**, *22,* 572.

[5] a) Q. Pei, G. Yu, C. Zhang, Y. Yang, A. J. Heeger, *Science* **1995**, *269*, 1086; b) K. M. Maness, R. H. Terrill, T. J. Meyer, R. W. Murray, R. M. Wightman, *J. Am. Chem. Soc*. **1996**, *118*, 10609; c) J. K. Lee, D. S. Yoo, E. S. Handy, M. F. Rubner, *Appl. Phys. Lett.* **1996**, *69*, 1686; d) J. Slinker, D. Bernards, P. L. Houston, H. D. Abruna, S. Bernhard, G. G. Malliaras, *Chem. Commun.* **2003**, 2392; e) A. B. Tamayo, S. Garon, T. Sajoto, P. I. Djurovich, I. M. Tsyba, R. Bau, M. E. Thompson, *Inorg. Chem*. **2005**, *44*, 8723; f) F. De Angelis, S. Fantacci, N. Evans, C. Klein, S. M. Zakeeruddin, J.-E. Moser, K. Kalyanasundaram, H. J. Bolink, M. Gratzel, M. K. Nazeeruddin, *Inorg. Chem.* **2007**, *46*, 5989; g) F. L. Zhang, L. Duan, J. Qiao, G. F. Dong, L. D. Wang, Y. Qiu, *Organic Electronics* **2012,** *13*, 2442.

[6] Reviews: a) R. D. Costa, E. Orti, H. J. Bolink, F. Monti, G. Accorsi, N. Armaroli, *Angew. Chem. Int. Ed. Engl.* **2012**, *51*, 8178; b) T. Hu, L. Duan, Y. Qiu, *J. Mater. Chem*. **2012**, *22*, 4206; c) S. Ladouceur, E. Zysman-Colman, *Eur. J. Inorg. Chem*. **2013**, 2985.

[7] a) G. Kalyuzhny, M. Buda, J. McNeill, P. Barbara, A. J. Bard, *J. Am. Chem. Soc.* **2003**, *125*, 6272; b) J. D. Slinker, J.-S. Kim, S. Flores-Torres, J. H. Delcamp, H. D. Abruna, R. H. Friend, G. G. Malliaras, *J. Mater. Chem*. **2007**, *17*, 76; c) L. J. Soltzberg, J. Slinker, S. Flores-Torres, D. Bernards, G. G. Malliaras, H. D. Abruna, J. S. Kim, R. H. Friend, M. D. Kaplan, V. Goldberg, *J. Am. Chem. Soc*. **2006**, *128*, 7761.

[8] a) H. J. Bolink, E. Coronado, R. D. Costa, E. Ortí, M. Sessolo, S. Graber, K. Doyle, M. Neuburger, C. E. Housecroft, E. C. Constable, *Adv. Mater*. **2008**, *20*, 3910; b) R. D. Costa, E. Ortí, H. J. Bolink, S. Graber, C. E. Housecroft, M. Neuburger, S. Schaffner, E. C.

Constable, *Chem. Commun.* **2009**, 2029; c) R. D. Costa, E. Ortí, H. J. Bolink, S. Graber, S. Schaffner, M. Neuburger, C. E. Housecroft, E. C. Constable, *Adv. Funct. Mater.* **2009**, *19*, 3456; d) R. D. Costa, E. Ortí, H. J. Bolink, S. Graber, C. E. Housecroft, E. C. Constable, *Adv. Funct. Mater.* **2010**, *20*, 1511; e) R. D. Costa, E. Ortí, H. J. Bolink, S. Graber, C. E. Housecroft, E. C. Constable, *J. Am. Chem. Soc.* **2010**, *132*, 5978; f) R. D. Costa, E. Ortí, H. J. Bolink, S. Graber, C. E. Housecroft, E. C. Constable, *Chem. Commun.* **2011**, *47*, 3207; g) A. M. Bünzli, H. J. Bolink, E. C. Constable, C. E. Housecroft, M. Neuburger, E. Ortí, A. Pertegás, J. A. Zampese, *Eur. J. Inorg. Chem*. **2012**, 3780; h) R. D. Costa, E. Ortí, D. Tordera, A. Pertegás, H. J. Bolink, S. Graber, C. E. Housecroft, L. Sachno, M. Neuburger, E. C. Constable, *Adv. Energy Mater.* **2011**, *1*, 282.

[9]   L. He, L. Duan, J. Qiao, D. Zhang, L. Wang, Y. Qiu, *Chem. Commun*. **2011**, *47*, 6467.

[10]   G-G. Shan, H-B. Li, D-X. Zhu, Z-M. Su, Y. Liao, *J. Mater. Chem.* **2012**, *22*, 12736.

[11]   L. Sun, A. Galan, S. Ladouceur, J. D. Slinker, E. Zysman-Colman, *J. Mater. Chem*. **2011**, *21*, 18083.

[12]   A. J. Wilkinson, H. Puschmann, J. A. K. Howard, C. E. Foster, J. A. G. Williams, *Inorg Chem.* **2006**, *45*, 8685.

[13]   a) S. Sprouse, K. A. King, P. J. Spellane, R. J. Watts, *J. Am. Chem. Soc.* **1984**, *106*, 6647; b) G. G. Shan, D. X. Zhu, H. B. Li, P. Li, Z. Su, Y. Liao, *Dalton Trans.* **2011**, *40*, 2947; c) L. He, J. Qiao, L. Duan, G. Dong, D. Zhang, L. Wang, Y. Qiu, *Adv. Funct. Mater.* **2009**, *19*, 2950.

[14]   H. T. Cao, G. G. Shan, B. Zhang, P. Li, S. L. Sun, Z. M. Su, *J. Mol. Struct.* **2012**, 1029.

[15]   a) N. Francesco, L. D. Massimo, C. Alessandra, B. Anna, P. Fausto, C. Sebastiano, *Organometallics* **2004**, *23*, 5856; b) G. G. Shan, H. B. Li, H. T. Cao, D. X. Zhu, P. Li, Z. M. Su, Y. Liao, *J. Organomet. Chem.* **2012**, *713*, 20.

[16]   a) N. Tian, D. Lenkeit, S. Pelz, L. H. Fischer, D. Escudero, R. Schiewek, D. Klink, O. J. Schmitz, L. González, M. Schäferling, E. Holder, *Eur. J. Inorg. Chem.* **2010**, 4875; b) C. S. Chin, M. S. Eum, S. Y. Kim, C. Kim, S. K. Kang, *Eur. J. Inorg. Chem.* **2007**, 372; c) N. M. Shavaleev, F. Monti, R. D. Costa, R. Scopelliti, H. J. Bolink, E. Ortí, G. Accorsi, N. Armaroli, E. Baranoff, M. Grätzel, M. K. Nazeeruddin, *Inorg. Chem.* **2012,** *51,* 2263; d) J. Li, P. I. Djurovich, B. D. Alleyne, M. Yousufuddin, N. N. Ho, J. C. Thomas, J. C. Peters, R. Bau, M. E. Thompson, *Inorg. Chem.* **2005,** *44,* 1713.

[17]   C. Dragonetty, L. Falciola, P. Mussini, S. Righetto, D. Roberto, R. Ugo, A. Valore, F.

DeAngelis, S. Fantacci, A. Sgamellotti, M. Ramon, M. Muccini, *Inorg. Chem.* **2007**, *46*, 8533.

[18] J. I. Goldsmith, W. R. Hudson, M. S. Lowry, T. H. Anderson, S. Bernhard, *J. Am. Chem. Soc.* **2005**, *127,* 7502.

[19] C. Rothe, C-J. Chiang, V. Jankus, K. Abdullah, X. Zeng, R. Jitchati, A. S. Batsanov, M. R. Bryce, A. P. Monkman, *Adv. Funct. Mater.* **2009**, *19,* 2038.

[20] S. T. Parker, J. Slinker, M. S. Lowry, M. P. Cox, S. Bernhard, G. G. Malliaras, *Chem. Mater.* **2005**, *17*, 3187.

[21] J. Zhang, L. Zhou, H. A. Al-Attar, K. Z. Shao, L. Wang, D. X. Zhu, Z. M. Su, M. R. Bryce, A. P. Monkman, *Adv. Funct. Mater.* **2013**, *23,* 4667.

[22] M. Nonoyama, *Bull. Chem. Soc. Jpn.* **1974**, *47*, 767.

[23] G. M. Sheldrick, SHELXL-97, Program for Crystal Structure Refinement, University of Gottingen, 1997.

[24] L. J. Farrugia, WINGX, A Windows Program for Crystal Structure Analysis, University of Glasgow, Glasgow, U.K., 1988.

[25] a) C. Lee, W. Yang, R. G. Parr, *Phys. Rev. B* **1998**, *37*, 785; b) A. D. Becke, *J. Chem. Phys.* **1993**, *98*, 5648.

[26] M. J. Frisch, G. W. Trucks, H. B. Schlegel, G. E. Scuseria, M. A. Robb, J. R. Cheeseman, G. Scalmani, V. Barone, B. Mennucci, G. A. Petersson, H. Nakatsuji, M. Caricato, X. Li, H. P. Hratchian, A. F. Izmaylov, J. Bloino, G. Zheng, J. L. Sonnenberg, M. Hada, M. Ehara, K. Toyota, R. Fukuda, J. Hasegawa, M. Ishida, T. Nakajima, Y. Honda, O. Kitao, H. Nakai, T. Vreven, J. A. Montgomery, Jr., J. E. Peralta, F. Ogliaro, M. Bearpark, J. J. Heyd, E. Brothers, K. N. Kudin, V. N. Staroverov, R. Kobayashi, J. Normand, K. Raghavachari, A. Rendell, J. C. Burant, S. S. Iyengar, J. Tomasi, M. Cossi, N. Rega, J. M. Millam, M. Klene, J. E. Knox, J. B. Cross, V. Bakken, C. Adamo, J. Jaramillo, R. Gomperts, R. E. Stratmann, O. Yazyev, A. J. Austin, R. Cammi, C. Pomelli, J. W. Ochterski, R. L. Martin, K. Morokuma, V. G. Zakrzewski, G. A. Voth, P. Salvador, J. J. Dannenberg, S. Dapprich, A. D. Daniels, Ö. Farkas, J. B. Foresman, J. V. Ortiz, J. Cioslowski, D. J. Fox, Gaussian 09W, revision A.02. Wallingford CT: Gaussian, Inc.; 2009.